Immunodeficiencies and autoimmunity

Clinical

Research Article

Antigen-driven PD-1+TOX+BHLHE40+ and PD-1+TOX+EOMES+ T lymphocytes regulate juvenile idiopathic arthritis *in situ*

Patrick Maschmeyer[1] , *Gitta Anne Heinz*[1]* , *Christopher Mark Skopnik*[2]* , *Lisanne Lutter[3]*, *Alessio Mazzoni[4]*, *Frederik Heinrich[1]*, *Sae Lim von Stuckrad[5,6]*, *Lorenz Elias Wirth[1]*, *Cam Loan Tran[1]*, *René Riedel[1]*, *Katrin Lehmann[1]*, *Imme Sakwa[1]*, *Rolando Cimaz[7,8]*, *Francesco Giudici[9]*, *Marcus Alexander Mall[5,10]*, *Philipp Enghard[2]*, *Bas Vastert[3]*, *Hyun-Dong Chang[1]*, *Pawel Durek[1,11]*, *Francesco Annunziato[4]*, *Femke van Wijk[3]*, *Andreas Radbruch**[1]* , *Tilmann Kallinich**[1,5,10]* and *Mir-Farzin Mashreghi**[1,11]*

[1] Deutsches Rheuma-Forschungszentrum (DRFZ), Institute of the Leibniz Association, Berlin, Germany
[2] Charité - Universitätsmedizin Berlin, corporate member of Freie Universität Berlin, Humboldt-Universität zu Berlin, and Berlin Institute of Health, Department of Nephrology and Intensive Care Medicine, Berlin, Germany
[3] Center for Translational Immunology, Wilhelmina Children's Hospital, University Medical Center Utrecht, Utrecht University, Utrecht, Netherlands
[4] Department of Experimental and Clinical Medicine and DENOTHE Center, University of Florence, Florence, Italy
[5] Charité - Universitätsmedizin Berlin, corporate member of Freie Universität Berlin, Humboldt-Universität zu Berlin, and Berlin Institute of Health, Department of Pediatric Pulmonology, Immunology and Critical Care Medicine, Berlin, Germany
[6] Charité - Universitätsmedizin Berlin, corporate member of Freie Universität, Humboldt-Universität zu Berlin, and Berlin Institute of Health, Berlin SPZ (Center for Chronically Sick Children), Berlin, Germany
[7] Anna Meyer Children's Hospital and University of Florence, Florence, Italy
[8] Department of Clinical Sciences and Community Health, University of Milano, Milano, Italy
[9] Department of Experimental and Clinical Medicine, University of Florence, Florence, Italy
[10] Berlin Institute of Health (BIH), Berlin, Germany
[11] BCRT/DRFZ Single-Cell Laboratory for Advanced Cellular Therapies - Brandenburg Center for Regenerative Therapies (BCRT), Berlin, Germany

T lymphocytes accumulate in inflamed tissues of patients with chronic inflammatory diseases (CIDs) and express pro-inflammatory cytokines upon re-stimulation *in vitro*. Further, a significant genetic linkage to MHC genes suggests that T lymphocytes play an important role in the pathogenesis of CIDs including juvenile idiopathic arthritis (JIA). However, the functions of T lymphocytes in established disease remain elusive. Here we dissect the transcriptional and the clonal heterogeneity of synovial T lymphocytes in JIA patients by single-cell RNA sequencing combined with T cell receptor profiling on the same cells. We identify clonally expanded subpopulations of T lymphocytes expressing genes reflecting recent activation by antigen *in situ*. A PD-1+TOX+EOMES+ population of CD4+ T lymphocytes expressed immune regulatory genes and chemoattractant genes for myeloid cells. A PD-1+TOX+BHLHE40+ population of CD4+, and a mirror population of CD8+ T lymphocytes expressed genes driving inflammation, and genes supporting B lymphocyte activation *in situ*. This analysis points out that multiple types of T lymphocytes have to be targeted for therapeutic regeneration of tolerance in arthritis.

Correspondence: Dr. Mir-Farzin Mashreghi
e-mail: mashreghi@drfz.de; pawel.durek@drfz.de

*Equal second authorship.
**Equal senior authorship.

⌨ Additional supporting information may be found online in the Supporting Information section at the end of the article.

Introduction

Chronic inflammatory diseases (CIDs), such as juvenile idiopathic arthritis (JIA) or inflammatory bowel disease (IBD), cannot be cured by current therapies and represent a major burden for public health [1–3]. T memory cells have been proposed to be critical drivers of CIDs, since (i) multiple alleles that are associated with these diseases are linked to genes that influence T cell activation and (ii), since T cells accumulate in chronically inflamed tissues of CID patients [4–11].

In the past, mostly CD4$^+$ T helper (T$_h$) cells have been implicated in driving CIDs, due to the expression of pro-inflammatory cytokines, among which GM-CSF and IL-21 have been especially associated with driving inflammation by activation of myeloid cells and B cells, respectively [12, 13]. While inhibition of GM-CSF showed positive outcomes in clinical trials in the adult form of arthritis, the global molecular signature for targeting the cells expressing such pro-inflammatory mediators *in situ* has not been identified [14–18]. Most studies so far have investigated pathogenic T cells in human CIDs by cytokine secretion only following re-stimulation *in vitro*. However, since most memory T lymphocytes are prone to respond to re-stimulation by secretion with cytokines, this approach misses the aim to particularly identify the pathogenic subsets of T$_h$ cells that respond to antigenic stimulation by secretion of cytokines *in vivo*.

At this point in time, technologies and algorithms to predict cognate antigens from the sequences of T cell receptors are being developed [19–22]. This approach might be revolutionary to identify putative (auto)antigens driving chronic inflammation as long as the antigen receptor sequences on pro-inflammatory T lymphocytes have been identified. Thus, targeting the (auto)antigens or the (auto)antigen-driven T lymphocytes maintaining chronic inflammation might be achieved by first linking the phenotype and the clonal identity of disease-driving T cells on the single-cell level.

Here, we aimed at identifying pathogenic cells among CD4$^+$ and CD8$^+$ T memory lymphocytes in chronically inflamed joints of JIA patients that have been activated by antigens *in situ*. By utilizing RNA sequencing combined with T cell receptor (TCR) profiling on the single-cell level, we discovered functionally antagonistic subpopulations of antigen-stimulated T lymphocytes that drive and regulate inflammation, respectively. We also uncovered their migratory behavior and their plasticity while being exposed to the inflammatory environment, as well as their molecular fingerprints for the selective targeting of pathogenic T memory lymphocytes driving chronic inflammatory diseases such as JIA.

Results and Discussion

Transcriptional landscapes of antigen-experienced T cells in inflamed joints of JIA patients

Here we have analyzed CD4$^+$CD45RO$^+$CD25$^-$, CD4$^+$CD45RO$^+$CD127^{lo}CD25$^+$, and CD8$^+$CD45RO$^+$ T lymphocytes, representing antigen-experienced conventional CD4$^+$ T lymphocytes (Tcon), regulatory CD4$^+$ T lymphocytes (Treg) and CD8$^+$ T lymphocytes, respectively. Cells were isolated from synovial fluid (SF) and peripheral blood (PB) of 7 patients with oligoarticular JIA by fluorescence-activated cell sorting (FACS) before single-cell transcriptomes and T cell receptor repertoires were determined by RNA-sequencing (Supporting Information Fig. S1A and B; Supporting Information Table 1). We had shown before that the isolation procedure used here does not affect gene expression of the isolated T cells, thus, these transcriptomes reflect gene expression *in vivo* [23, 24]. We performed shared nearest neighbor-clustering based on the transcriptional profiles of these cells and projected the resulting clusters using dimensional reduction analysis by t-distributed stochastic neighbor embedding (t-SNE) [25]. Most of the 74 891 cells of blood and synovia from all patients clustered according to their lineage and tissue origin (Fig. 1A).

Synovial Tcon from all patients combined were further clustered into six different subsets (clusters 0–5). All clusters were comprised of cells from each individual patient, except cluster 5, which did not include cells of patient 2 (Fig. 1B and C; Supporting Information Fig. S2). Transcriptomic signatures for the 6 synovial Tcon clusters were defined by 603 genes (Fig. 1D, Supporting Information Table 2). To characterize the clusters further, we analyzed their expression of functionally defined gene sets (modules) and individual signature genes (Fig. 1E and F, Supporting Information Table 3) [26]. Cluster 0 was the largest, comprising an average of 53.8% (range: 44.9%-60.4%) of the synovial Tcon (Fig. 1C). Cells of cluster 0 expressed a gene module typical for circulating naive or central memory T (T$_{CM}$) cells, including the signature genes *SELL*, *CCR7*, and *S1PR1* (Fig. 1E and F; Supporting Information Fig. S3) [27–29]. Cluster 1 comprised 17.6% (11.8%-24.25%) of the synovial Tcon (Fig. 1C). These cells expressed a gene module indicating activation by antigen in the synovia *in situ*, including MHC class II genes and *CD40LG*, as well as genes encoding for cytokines, like *IFNG*, *TNF*, *CXCL13*, and *CSF2* (GM-CSF) (Fig. 1E and F; Fig. 3; Fig. S3) [30–34]. These cells also expressed a gene module characterizing tissue-resident memory (T$_{RM}$) cells, including expression of *CXCR6*, *DUSP6*, *ITGAE* (CD103), *ZNF683* (HOBIT), and downregulation of
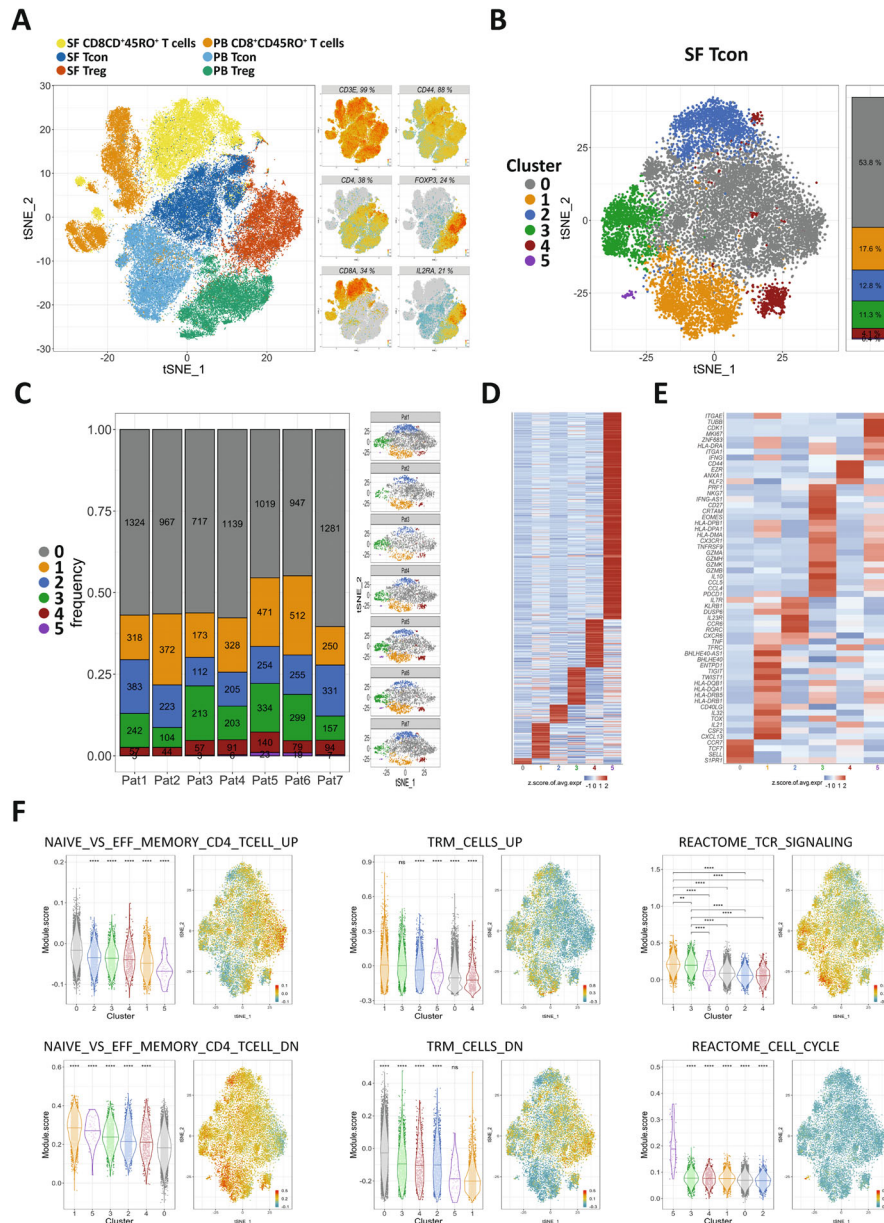
Figure 1. Transcriptional landscape of the antigen-experienced (memory) T cell compartment and heterogeneity of synovial CD4$^+$ Tcon in inflamed joints of JIA patients. CD4$^+$CD45RO$^+$CD25$^-$ Tcon, CD4$^+$CD45RO$^+$CD25$^+$ Treg and CD8$^+$CD45RO$^+$ T cells from the synovial fluid (SF) and the peripheral blood (PB) of JIA patients were flow cytometry-sorted prior to single-cell RNA sequencing (n = 7 for SF Tcon and SF CD8$^+$CD45RO$^+$ T cells; n = 6 for SF Treg, PB Treg, PB Tcon and PB CD8$^+$CD45RO$^+$ T cells).(A) A t-SNE map of pooled antigen-experienced T cells from the PB and the SF of the analyzed JIA patients is shown (n = 74 891 cells). Each dot represents a single cell and is colored according to the respective sorted population. (B) CD4$^+$ Tcon (n = 13 756 cells) from inflamed joints (SF) of 7 JIA patients were clustered and projected on a t-SNE map showing the formation of 6 different clusters (0-5). Each dot corresponds to a single cell and is colored according to its cluster affiliation. (C) Quantification and t-SNE projection of the cluster distribution among synovial Tcon of the 7 different JIA patients. The y-axis of the bar graph depicts the fraction of the clusters from (0-1), while numbers in bars show the absolute cell numbers of recorded Tcon of a particular cluster in each patient. (D) Heatmap showing the z-score normalized mean expression of 603 cluster-specific genes. (E) Heatmap showing the z-score normalized mean expression of selected T cell function-associated genes. (F) Module scores of gene sets associated to previously described T cell functions projected on t-SNE maps and statistical comparison between clusters illustrated as violin plots. In (D) and (E), heatmap color scales indicate row-wise z-scores of cluster-means of log-normalized expression values. Signature genes were tested for significant differential expression by cells of a cluster in comparison to cells from all other clusters by a two-sided unpaired Wilcoxon rank sum test with Bonferroni correction. Cutoff was a minimum of 5% expressing cells in the respective cluster and an adjusted *p*-value ≤ 0.05. In (F) A two-sided unpaired Wilcoxon test with ns *p* > 0.05; *p ≤ 0.05; **p ≤ 0.01; ***p ≤ 0.001 and ****p ≤ 0.0001 was used. The gene set NAIVE_VS_EFF_MEMORY_CD4_TCELL_UP (GSE11057) contains genes, whose expression have been found to be upregulated in naive CD4$^+$ T cells as opposed to effector memory T cells. The gene set NAIVE_VS_EFF_MEMORY_CD4_TCELL_DN (GSE11057) contains genes, whose expression have been found to be downregulated in naive CD4$^+$ T cells as opposed to effector memory T cells. Analogously TRM_CELLS_UP and TRM_CELLS_DN, are gene sets containing genes that were found to be upregulated or downregulated in T$_{RM}$ cells, respectively [35]. The curated REACTOME_TCR_SIGNALING (M15381) and REACTOME_CELL_CYCLE (M543) gene sets are from the Reactome database and contain genes that are associated with TCR signaling and with the cell cycle, respectively [32]. The particular genes of all used gene sets can be found in Supplementary Table 2.

KLF2 (Fig. 1E and F; Supporting Information Fig. S3) [29, 35-39]. Cells of cluster 2 made up for 12.8% (8.8%-16.5%) of synovial Tcon (Fig. 1C). These cells qualified as *bona fide* T_h17 cells due to the expression of *RORC*, *IL23R*, and *CCR6* (Fig. 1E; Supporting Information Fig. S3) [40]. A subset of these cells also expressed the T_RM-associated gene module (Fig. 1F), and the genes *CD40LG*, *TNF*, and *CSF2*, indicating their recent activation by antigen *in situ* (Figs. 1E and 3C) [33, 35]. Cells of cluster 3 accounted for an average of 10% (6.1%-16.7%) of synovial Tcon (Fig. 1C). These cells expressed the gene module of recently activated T cells (Fig. 1F, REACTOME_TCR_SIGNALING), and genes indicating T cell receptor (TCR) stimulation, in particular *TNFRSF9* (4-1BB, CD137), *CRTAM*, and MHC class II genes, but not *CD40LG* (Figs. 1E and 3; Supporting Information Fig. S3) [30–32, 41, 42]. They also expressed *EOMES* and/or *IL10* and/or *IFNG ex vivo*, resembling type 1 regulatory (Tr1)-like cells [43–45]. Cells of this cluster expressed gene modules of both circulating and T_RM cells (Fig. 1F), including the genes *S1PR1, CX3CR1* or *CXCR6* (Fig. 1E; Supporting Information Fig. S3) [35–38]. Cells of cluster 4 represented 4.1% (2.5%-6.2%) of synovial Tcon (Fig. 1C). These cells expressed high levels of *CD44, ANXA1* (ANNEXIN A1), and/or *EZR* (EZRIN; Fig. 1E; Supporting Information Fig. S3). Expression of these genes has been associated with survival, differentiation, and functional polarization of T cells [46–50]. Some of the cells of this cluster also expressed *CD40LG* and cytokine genes, such as *CSF2* or *TNF* (Figs. 1E and 3). Cells of cluster 5 were a minor population (0.4%; 0.0–1.0%) of synovial Tcon (Fig. 1C). They were proliferating *in situ*, as indicated by expression of the Reactome gene module "cell cycle" (Fig. 1F) and expression of genes like *CDK1* or *MKI67* (Fig. 1E) [32, 51-53].

The T cell receptor repertoire of synovial Tcon reveals clonal relationships between different subpopulations

For 61.4% of the individual synovial Tcon (8445 cells), we could also determine the full-length TCR α and ß chain sequences (Supplementary Table 4). A total of 5632 of these cells (66.7%) expressed a TCR detected only once, and 2813 cells (33.3%) expressed a TCR detected twice or more often (Fig. 2A). 512 (18.2%) of the detected expanded clones could be assigned to the 10 most abundant clonotypes, which possessed between 19 and 172 members (Fig. 2A). Cells of expanded clonotypes were most prevalent among cluster 1 (62.5 ± 14.2%), cluster 3 (41.7 ± 4.7%), and cluster 5, the latter in three of six of the patients only (Fig. 2A and B).

To define the relationship between different subpopulations of synovial Tcon, we compared their TCR repertoires and generated a transcriptional trajectory according to gene expression along a pseudotime dimension with the unsupervised inference method Monocle, which organizes trajectories according to the quantitative expression of signature genes [54]. We then projected the synovial Tcon clusters onto the trajectory (Fig. 2C and D; Supporting Information Fig. S4a). The resulting trajectory had a branched structure with four terminal nodes separated by two main compo-

nents, with component 1 (*x*-axis) being determined by TCR signaling (Fig. 2E) and component 2 (*y*-axis) being dominated by signature genes of the distal nodes, which were defined by clusters 0, 1, 2, and 3 of synovial Tcon (Fig. 2C; Supporting Information Fig. S4a).

Comparison of the TCR repertoires of the synovial Tcon clusters showed overlaps between cells of clusters 1 and 0 (34%), 1 and 2 (19%), 1 and 4 (17%), 1 and 5 (12%), 2 and 4 (13%), 2 and 5 (9%), 4 and 5 (6%), 5 and 0 (41%), as well as cells of clusters 5 and 3 (29%). These overlaps were significantly overrepresented compared to simulated randomized distributions of TCR sequences among the different clusters (Fig. 2F; Supporting Information Fig. S4b and Table 5). Integrating the repertoire relationships and the trajectory based on the expression of functional genes, a significant linkage of clusters 2, 4, and 1 became apparent. Shortest-Path analysis of the data suggested that T_h17-like cells of cluster 2 had differentiated via a transitional state, represented by cluster 4, into antigen-activated Tcon of cluster 1 (Fig. 2G), although cluster 1 also contained cells originating from clusters other than 2 and 4 (Supporting Information Fig. S4b). In summary, clonal expansion, clonal linkage between clusters, and a trajectory that is based on the expression of functional genes identify cells of clusters 1 and 3 as terminally differentiated, *in situ*-activated Tcon putatively driving chronic inflammation of the joint.

The population of synovial *PDCD1*^hi *TOX*+ Tcon consists of functionally distinct subsets

Few of the cells of clusters 1 and 3 expressed *MKI67* or *CDK1*, suggesting that most of them were no longer proliferating, and had been clonally expanded in the past (Fig. 1E and F, Supporting Information Fig. S3). Apart from the observed clonal expansion of Tcon from synovial clusters 1 and 3, those cells also expressed *TOX*, a gene indicating a history of repeated antigenic restimulation (Fig. 3B). Expression of *TOX* has been described to be induced by TCR stimulation in CD8+ T cells of a chronic infection mouse model, facilitating the survival of these cells [55–57]. The present analysis identifies the expression of *TOX* as a hallmark of distinct CD4+ T cells of chronically inflamed human tissue for the first time. Among the genes known to be induced by *TOX* are *TIGIT* and *PDCD1*, which were also expressed by cells of clusters 1 and 3 (Fig. 3B) [57]. This phenotype of "exhaustion" contrasted with their expression of genes encoding cytokines and chemokines (Fig. 3C). Indeed, the cells expressing *TOX* or *PDCD1* were the cells expressing functional genes encoding cytokines and chemokines (Supporting Information Fig. S5a and b). Quantitative PCR (qPCR) of flow-sorted synovial Tcon of JIA patients further confirmed that cells expressing the protein PD-1 also expressed higher levels of genes encoding for cytokines and chemokines than PD-1⁻ Tcon *in situ* (Supporting Information Fig. S5c). Moreover, synovial PD-1-expressing Tcon also expressed higher levels of *TWIST1* and *EOMES*, i.e., genes encoding transcription factors that actively regulate adaptation
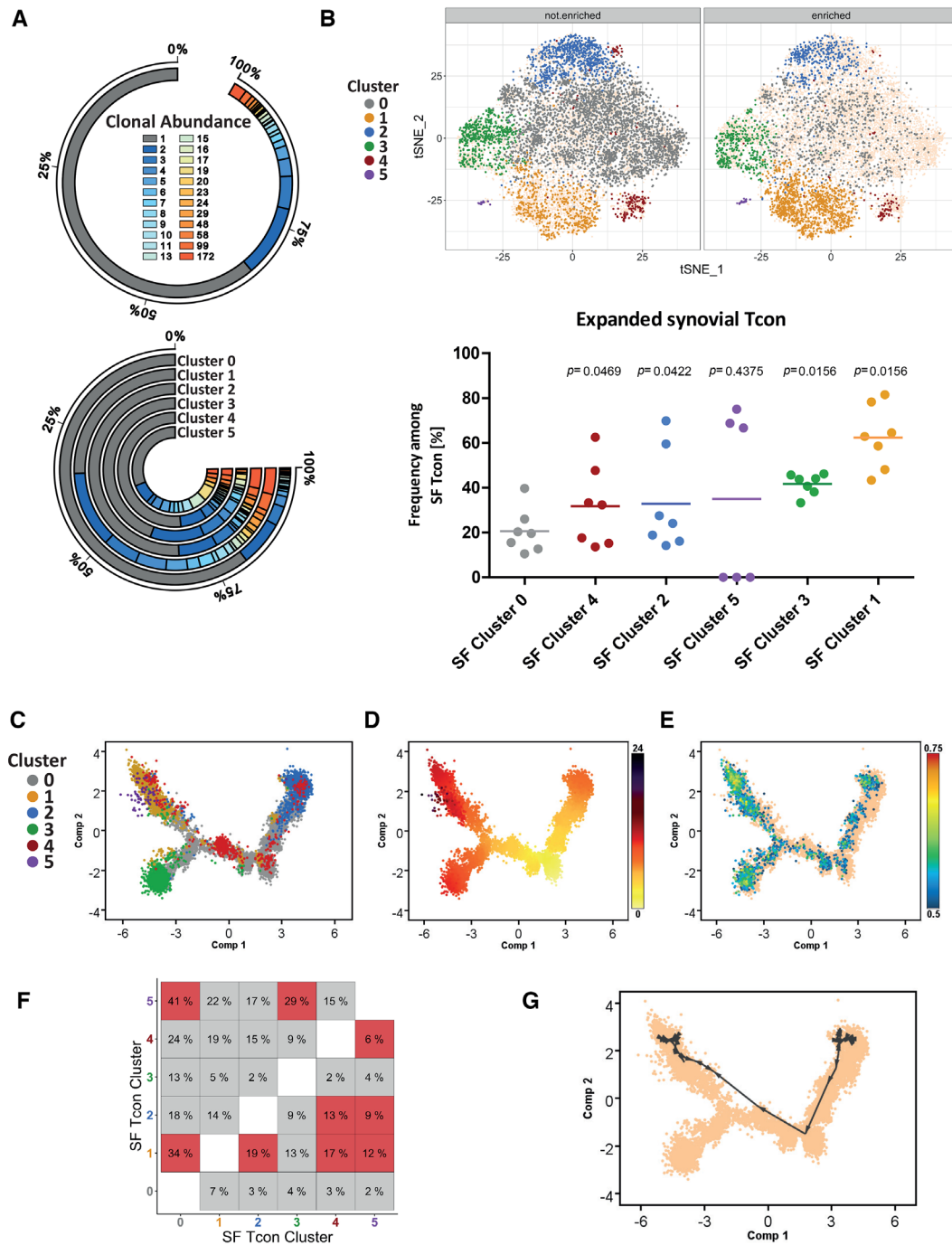
Figure 2. Clonal relationships of synovial Tcon reveals clusters 1 and 3 as clonally enriched and links cluster 1 to cluster 2 and 4. CD4$^+$CD45RO$^+$CD25$^-$ Tcon from the synovial fluid of 7 JIA patients were purified by flow cytometry prior to single-cell TCR profiling combined with single-cell transcriptome analyses. (A) Shown are detected frequencies of unique and expanded T cell clones among all synovial Tcon and in each cluster. The color-scale corresponds to the clonal abundance (i.e. number of clones) of synovial Tcon clonotypes. (B) Distribution of unique and expanded T cell clones among the t-SNE map of synovial Tcon as well as frequencies of expanded clones in each cluster. A two-sided paired Wilcoxon test was performed to determine significant differences between cluster 0 and each other cluster. Significance was assumed with a $p \leq$ 0.05. (C) and (D) Pseudotime-based gene expression arranges cells along a Monocle trajectory resulting in a branched structure of synovial Tcon. (C) Each cell is represented as one dot and labeled according to its affiliated cluster. (D) Each cell is colored according to its pseudotime value, which suggests a direction of Tcon development with a root in the lower right corner (dominated by cluster 0). (E) Projection of the REACTOME_TCR_SIGNALING (M15381) gene set on the trajectory. (F) Clonal overlaps between the different clusters of synovial Tcon (in percent). Highlighted in red are clonal overlaps that are significantly overrepresented compared to 1000 simulated randomized overlaps. (G) Shortest-Path analysis directed by clonal densities of Tcon clones that are present in all synovial clusters among the Monocle trajectory described in (C). In (B), (E) and (G), Cells that are not highlighted are depicted as yellow in the background to outline the shape of the t-SNE map and the trajectory, respectively. Shown are pooled CD4$^+$ Tcon (n = 13 756 cells) from inflamed joints of 7 JIA patients.
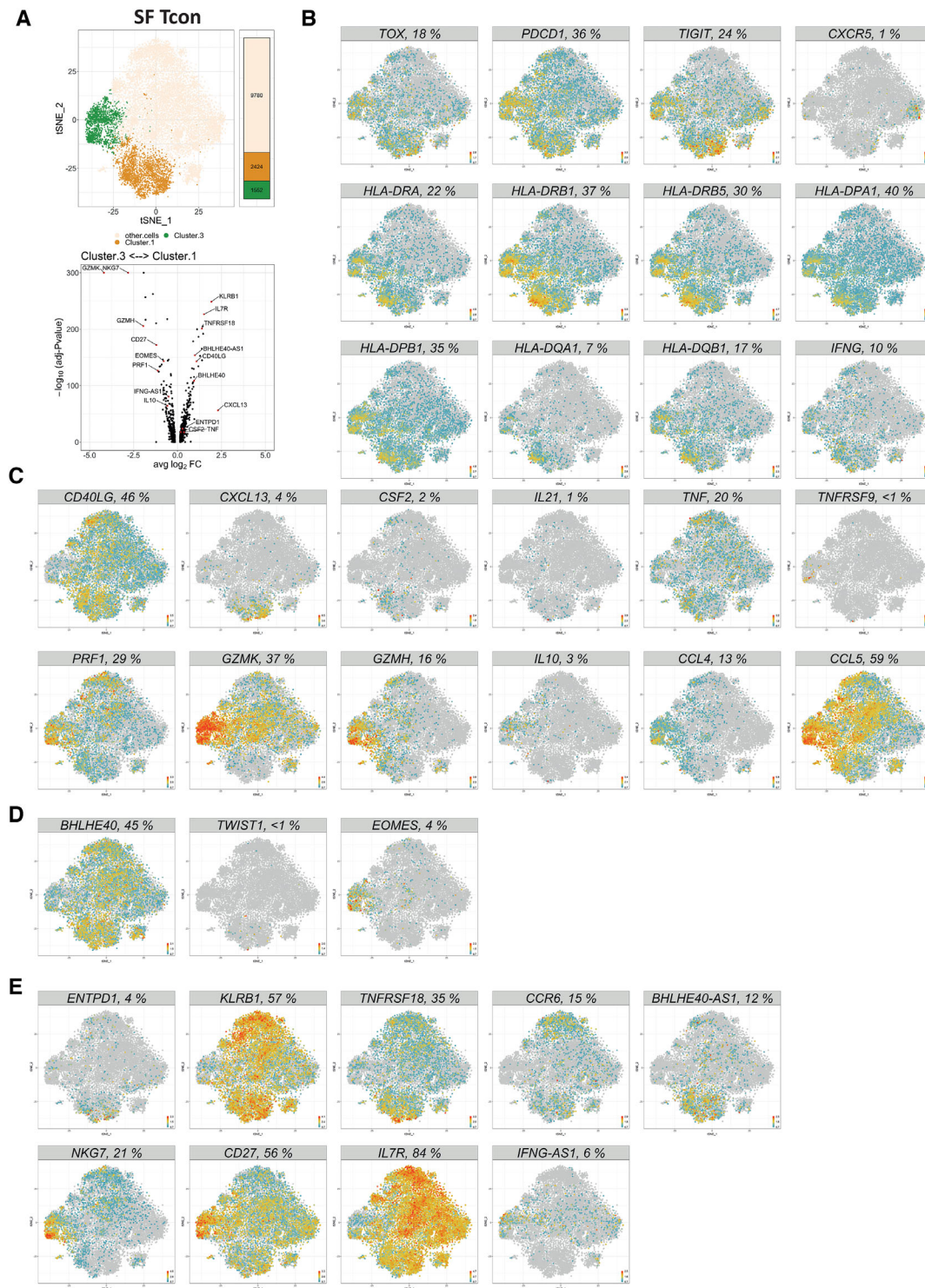
Figure 3. Subsets of antigen-stimulated $PDCD1^{hi}TOX^+$ synovial Tcon from JIA patients share a signature of activation but are distinct regarding their functional responses. SF Tcon of 7 JIA patients were purified and subjected to single-cell RNA-sequencing as described in Figure 1.(A) A t-SNE map highlighting synovial Tcon in clusters 1 and 3 and a volcano plot showing genes that are differentially expressed by cells in these clusters. Significance was determined by a two-sided unpaired Wilcoxon rank sum test with Bonferroni correction. Cutoff was a minimum of 5% expressing cells in either cluster. (A) Feature plots showing the expression of indicated genes whose expression (or absence thereof, e.g. $CXCR5$) are shared between cells of clusters 1 and 3. (C) Feature plots of indicated functional response genes that are differentially expressed between synovial Tcon of clusters 1 and 3. (D) Feature plots of indicated transcription factor genes that are differentially expressed between cells of synovial Tcon clusters 1 and 3. (E) Expression of indicated marker genes to distinguish between cells of clusters 1 and 3 among synovial Tcon. In (B)-(D) Percentages in header bars of feature plots display the frequencies of Tcon that express the indicated genes. Shown are pooled CD4$^+$ Tcon (n = 13 756 cells) from inflamed joints of 7 JIA patients.

of T cells to chronic inflammation and control the expression of cytotoxicity-associated molecules, respectively [58–63]. Of note, cells of both clusters 1 and 3 lacked *CXCR5* expression, resembling non-follicular peripheral T_h cells that have been nominated as prime candidates driving chronic inflammation in rheumatoid arthritis and celiac disease (Fig. 3A; Supporting Information Fig. S7b) [13, 64].

Despite their common expression of *TOX, PDCD1* and other genes indicating recent cognate activation, cells of clusters 1 and 3 differed fundamentally in their response to antigenic stimulation (Fig. 3A–C). Cells of cluster 1 expressed *CD40LG* and pro-inflammatory cytokine and chemokine genes, in particular *CSF2, TNF, IFNG, IL21*, and *CXCL13* (Fig. 3A and C; Supporting Information Fig. S5d). Some of these cells also expressed CD25 as a hallmark of recent activation *in situ*, since CD4+CD45RO+CD25+ T cells from the same synovia identified a cluster of FOXP3− T cells that resembled CD25− T cells of synovial cluster 1 with respect to expression of cytokines and chemokines (see cluster 2 of CD4+CD45RO+CD127loCD25+ T cells in Supporting Information Fig. S6 and Table 6). Interestingly, synovial Tcon cluster 1 displayed considerable heterogeneity in itself, since some cells expressed *CSF2* and *TNF*, indicating that these Tcon may support the activation of myeloid cells, while other cells rather expressed *IL21* and *CXCL13*, indicating their potential to attract and support B cell activation and differentiation (Fig. 3C) [65–68].

Tcon of synovial cluster 3 responded differently to antigenic stimulation *in situ* than Tcon of synovial cluster 1. They expressed *TNFRSF9* (4-1BB, CD137), *IL10, PRF1*, and genes encoding granzymes (Fig. 3A and C), i.e., genes associated with Tr1-like cells. Such cells have been reported to regulate immune reactions by IL-10, and to kill myeloid cells and activated T cells with granzymes [43–45, 69, 70]. Nevertheless, they may also support inflammation, since they expressed the chemokine genes *CCL4* and *CCL5* (Fig. 3C), with the potential to attract myeloid cells [71].

Cells of clusters 1 and 3 also differed fundamentally in their expression of key transcription factors. While cells of cluster 1 expressed *BHLHE40* and *TWIST1*, cells of cluster 3 expressed *EOMES* (Fig. 3D; Fig. S7A). *TWIST1* is selectively upregulated in CD4+ T cells upon repeated antigenic stimulation and enhances expression of genes promoting the persistence of the cells in the inflammatory environment [61–63]. Thirty-four of the 41 synovial Tcon that expressed *TWIST1* belonged to cluster 1 (Fig. 3D). While *TWIST1*+ cells were sparsely detectable by single-cell sequencing, *TWIST1* expression was readily detectable by qPCR of flow-sorted synovial Tcon of cluster 1 (Supporting Information Fig. S7a). Of note, expression levels of *TWIST1* in T cells are dependent on TCR activation and already decline rapidly 3 h after onset of activation, highlighting cells that had been stimulated by antigen within 3 h before biopsy [58]. Cells of cluster 1 also expressed the gene encoding BHLHE40 (Fig. 3A and D). This transcription factor has been associated with the expression of pro-inflammatory cytokines (e.g., GM-CSF), and with the suppression of immuno-regulatory genes [72–75]. This is in line with the expression pattern we observe here for synovial Tcon of cluster 1. Finally,

in line with the functional genes expressed by Tr1-like Tcon of synovial cluster 3 (Fig. 3A–C; Supporting Information Fig. S5a and b), these cells expressed the transcription factor *EOMES*, which has been reported to control the differentiation of Tr1-like cells (Fig. 3D) [43, 44].

Apart from the genes discussed so far, Tcon of synovial clusters 1 and 3 differentially expressed other genes. Cells of cluster 1 expressed *ENTPD1* (CD39), *KLRB1* (CD161), *CCR6, TNFRSF18* (GITR), and the long-non-coding RNA *BHLHE40-AS1* (Fig. 3E). Cells of cluster 3 did not express *IL7R*, but *CD27, NKG7*, and the long-non-coding RNA *IFNG-AS1* (Fig. 3E). These genes may serve in the future to identify and characterize such cells in the pathological context.

PD-1 and CD39 and/or CD161 were sufficient to identify and discriminate synovial CD4+ T cells of clusters 1 and 3 in JIA (Supporting Information Fig. S7). Comparing expression of the genes *CXCL13, IL21, CSF2, TWIST1, IFNG, BHLHE40AS1, IL10*, and *EOMES* of PD-1+CD39− and PD-1+CD39+ synovial CD4+ T cells confirmed the gene expression patterns observed by single-cell RNA-sequencing (Supporting Information Fig. S7). In addition, flow cytometric analysis showed that PD-1highCXCR5−CD4+ T cells accumulated in the inflamed joints of JIA patients and that the dichotomy of these cells remained stable after re-stimulation *in vitro* (Fig. S7b-e). Pro-inflammatory PD1highCD4+ T cells expressing CD39 and/or CD161 secreted the cytokines GM-CSF and IL-21, while EOMES+ Tr1-like cells secreted IL-10 (Fig. S7b-e). Mutually exclusive expression of CD161 and CD39 versus EOMES among T_h cells and the accumulation of CD161+CD4+ T cells was observed not only for inflamed joints of JIA, but also for inflamed intestines of patients with IBD (i.e. Crohn´s disease and ulcerative colitis), suggesting that PD1highCD39+/CD161+ and PD1highEOMES+CD4+ T cells dictate the phenotype of inflammation in various tissues of distinct CIDs (Supporting Information Fig. S8a-c).

Tr1-like cells of synovial Tcon cluster 3 are circulating in the peripheral blood of JIA patients

While pro-inflammatory Tcon of synovial cluster 1 expressed only gene modules and signature genes of T_{RM} cells, synovial Tr1-like Tcon of cluster 3 showed expression of genes associated both with resident and circulating T cells (Fig. 1E and F; Supporting Information Fig. S3). Accordingly, we detected Tcon in the peripheral blood of JIA patients that resembled synovial Tr1-like cells of cluster 3. For this, we analyzed the single-cell transcriptomes and TCR repertoires of blood-circulating CD4+CD45RO+CD25− Tcon from six of the seven JIA. Analysis of the transcriptomes from blood Tcon separated these cells into seven different subsets (clusters 0–6) among which 402 genes were specifically expressed (Fig. 4A-C and Supporting Information Table 7). TCR repertoire analyses of CD4+ Tcon from the blood and from inflamed synovia showed that blood-circulating Tcon possessed a reduced abundancy of expanded clones compared to synovial Tcon (Fig. 4D; Supporting Information Fig. S9a and Table 8). This analysis also revealed that CD4+ Tcon of blood cluster 5 harbored the highest frequency of
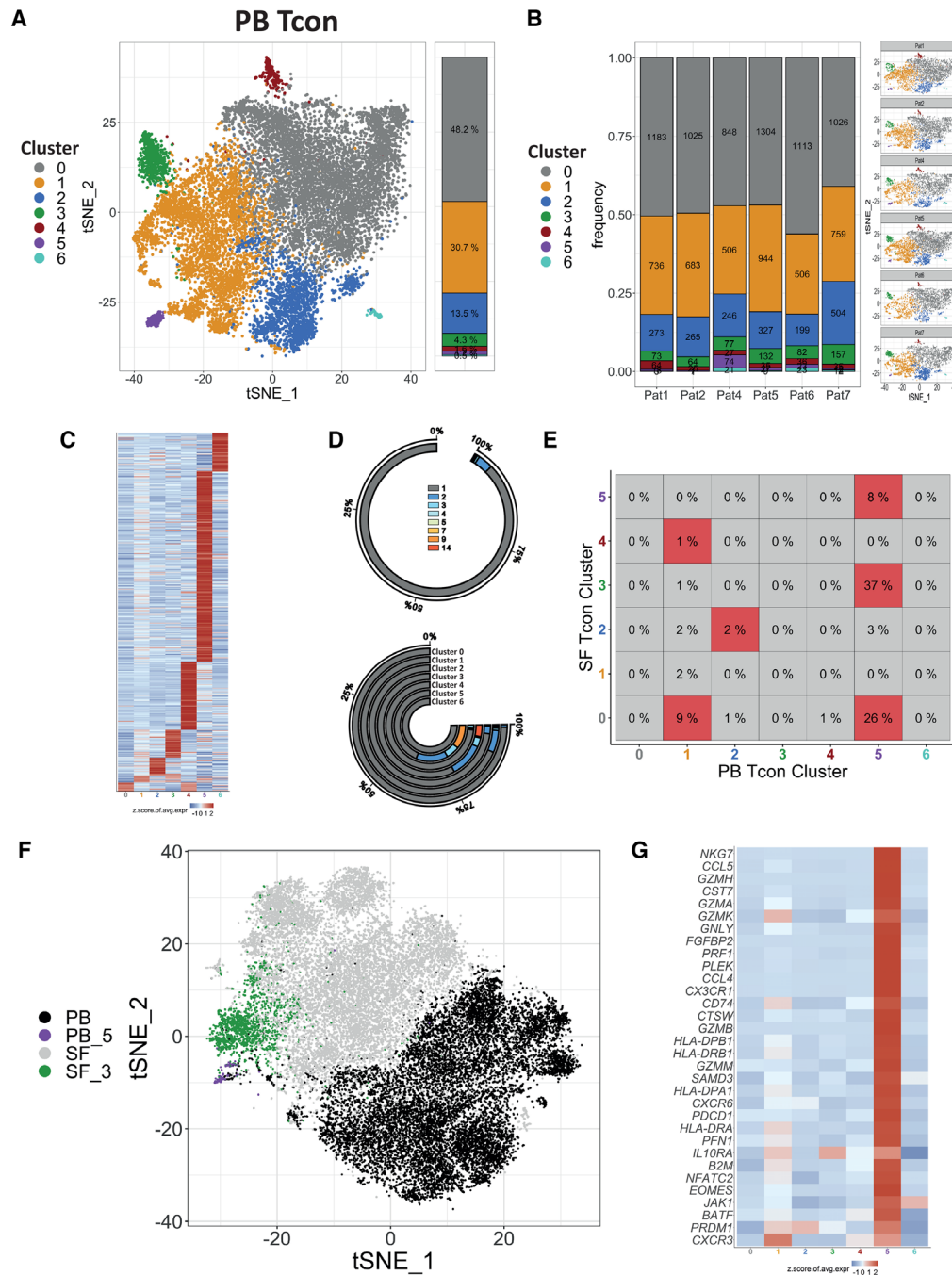
Figure 4. Tr1-like cells from synovial Tcon cluster 3 of inflamed joints are circulating in the peripheral blood of JIA patients. Single-cell transcriptomes and TCR expression of PB and SF Tcon from JIA patients were analyzed following purification by flow cytometry. (A) Cluster analysis and t-SNE projection of 13 479 Tcon from the PB of 6 JIA patients. Each dot represents a single cell and is colored according to its affiliation to one of the 7 identified clusters (clusters 0–6). (B) Quantification and t-SNE projections of clusters among the individual JIA patients. (C) Heatmap showing the z-score normalized mean expression of 402 cluster-specific genes. (D) Detected frequencies of unique and expanded T cell clones among all circulating PB Tcon and in each PB Tcon cluster. The color-scale corresponds to the clonal abundance (i.e. number of clones) of PB Tcon clonotypes. (E) Clonal overlaps between the different clusters of synovial and PB Tcon (in percent). Highlighted in red are clonal overlaps that are significantly overrepresented compared to 1000 simulated randomized overlaps. (F) Combined t-SNE map of Tcon from the PB and the SF. Each dot represents a cell. Displayed are cells from PB Tcon cluster 5 (violet), PB Tcon from all clusters except cluster 5 (black), SF cluster 3 (green) and Tcon from all SF clusters except from cluster 3 (grey). (G) Heatmap displaying genes that are expressed by circulating Tr1-like cells found in PB cluster 5 representing a molecular fingerprint for the identification of SF-derived cells in the PB. In (C) and (G) Heatmap color scales indicate row-wise z-scores of cluster-means of log-normalized expression values. Signature genes were tested for significant differential expression by cells of a cluster in comparison to cells from all the other clusters by a two-tailed unpaired Wilcoxon rank sum test with Bonferroni correction. Cutoff was a minimum of 5% expressing cells in the respective cluster and an adjusted *p*-value ≤ 0.05. Shown are pooled CD4$^+$ Tcon (n = 13 479 cells) from PB of 6 JIA patients.
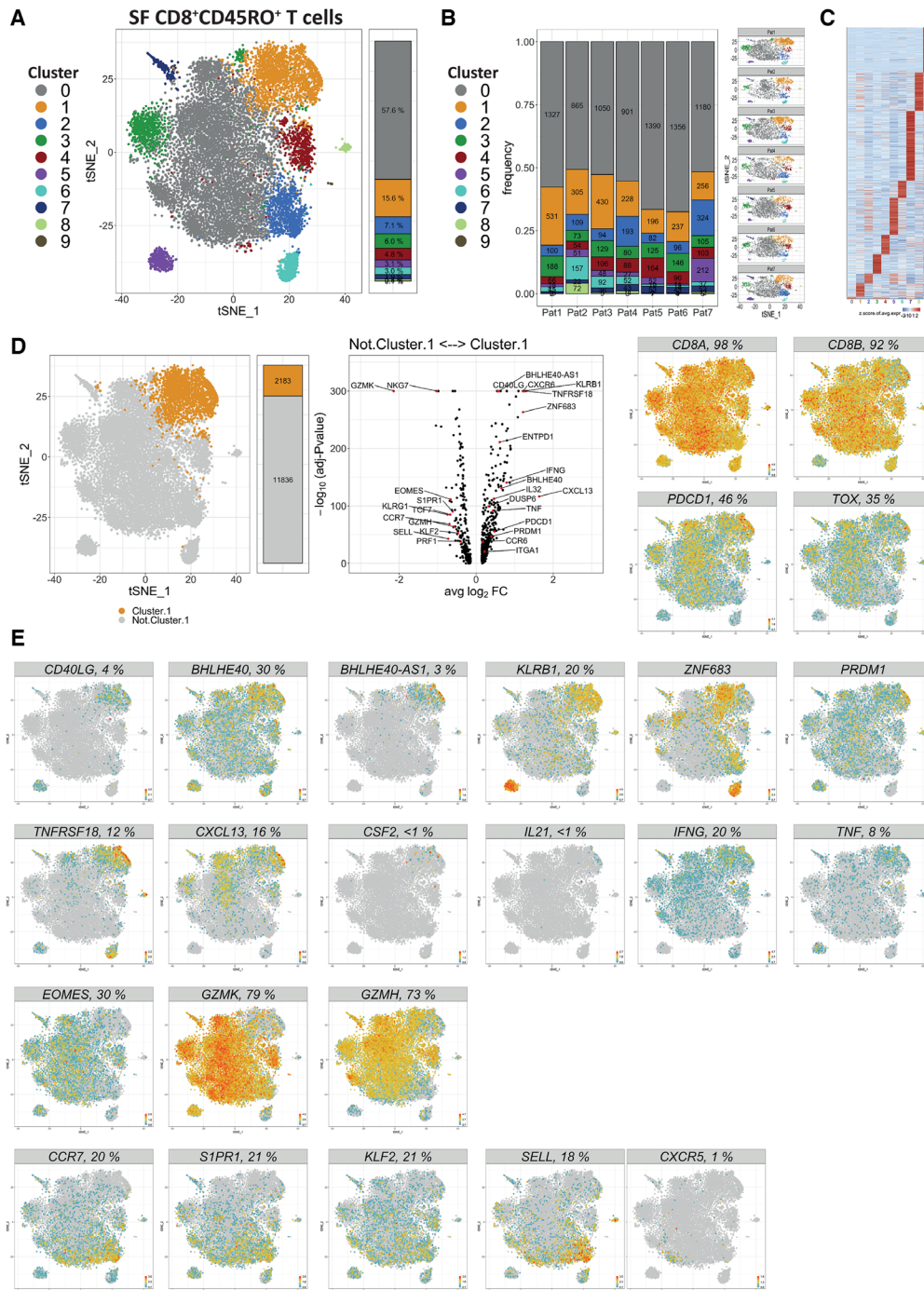
Figure 5. A subset of antigen-experienced (memory) CD8$^+$ T cells resembles pro-inflammatory T helper cells in the inflamed joints of JIA patients and expresses a T$_{RM}$ cell gene signature. CD8$^+$CD45RO$^+$ T cells from the SF of 7 JIA patients were purified by flow cytometry to determine their transcriptomes by RNA single-cell sequencing.(A) 14 019 CD8$^+$CD45RO$^+$ T cells from inflamed joints of 7 JIA patients were sequenced, clustered and projected onto a t-SNE map. Clustering separated them into 10 different subsets (clusters 0–9). Each dot represents a single cell and is colored according to its cluster affiliation. (B) Quantification and t-SNE projections of the cluster distributions among individual patients. (C) Heatmap showing the z-score normalized mean expression of 851 cluster-specific genes. (D) Volcano plot summarizing differentially expressed genes of CD8$^+$CD45RO$^+$ T cells in synovial cluster 1, as compared to synovial CD8$^+$CD45RO$^+$ T cells that are not present in cluster 1. In addition, a t-SNE map showing the groups with the cells that were compared and feature plots depicting the expression of *CD8A*, *CD8B*, *PDCD1* and *TOX* are shown. Significance was determined by a two-sided unpaired Wilcoxon rank sum test with Bonferroni correction. Cutoff was a minimum of 5% expressing cells in either cluster. (E) Feature plots showing the expression of indicated genes whose expression is up- or downregulated by cells of SF CD8$^+$CD45RO$^+$ T cells in cluster 1. In (C), heatmap color scales indicate row-wise z-scores of cluster-means of log-normalized expression values. Signature genes were tested for significant differential expression by cells of a cluster in comparison to cells from all other clusters by a two-sided unpaired Wilcoxon rank sum test with Bonferroni correction. Cutoff was a minimum of 5% expressing cells in the respective cluster and an adjusted *p*-value ≤ 0.05. Shown are pooled CD8$^+$CD45RO$^+$ T cells from inflamed joints (n = 14 019 cells) of 7 JIA patients.

expanded CD4$^+$ Tcon clones among all blood clusters, as well as clones that overlap with CD4$^+$ Tcon clones of paired synovial fluid samples (Fig. 4D; Supporting Information Fig. S9b). Of note, Tcon of blood cluster 5 specifically recapitulated the antigen receptor repertoire of synovial Tcon cluster 3, in that 37% of clones were shared between cells of both clusters in the 6 patients from whom we received both blood and synovial fluid (Fig. 4E and Supplementary Table 9). Accordingly, Tcon of blood cluster 5 localized next to Tcon of synovial cluster 3 in a combined t-SNE map, displaying the similarity of their transcriptomes (Fig. 4F). Tcon of blood cluster 5 indeed was highly similar to Tcon of synovial cluster 3 and expressed functional molecules of these Tr1-like cells, including *EOMES, PRF1*, granzymes, and *PDCD1* (Fig. 4G). However, they did not express *IL10 in situ* (Supporting Information Fig. S9c). This may indicate that the circulating cells had not recently been activated by (synovial) antigens or lacked recent exposure to additional factors specifically found in inflamed tissues. Tcon of blood cluster 5, with their Tr1-like transcriptome, might define a novel immunoregulatory mechanism preventing systemic spread of inflammation and confining inflammation to distinct joints in oligoarthritis.

A subset of antigen-experienced CD8$^+$ T cells resembles synovial CD4$^+$ T$_h$ cells of cluster 1

Apart from Tcon, also CD8$^+$ T memory cells have been implicated earlier in the pathogenesis of JIA [76]. Here we originally identified a prominent cluster of synovial CD8$^+$ T cells with transcriptomes resembling those of pro-inflammatory synovial CD4$^+$ T$_h$ cells of cluster 1. Synovial CD8$^+$CD45RO$^+$ T lymphocytes of all 7 JIA patients robustly and reproducibly clustered into 10 different populations (clusters 0–9; Fig. 5A). Their frequencies were between 0.1% and 57.6% of the 14 019 synovial CD8$^+$CD45RO$^+$ T lymphocytes and were defined by 851 differentially expressed signature genes (Fig. 5B and C; Supporting Information Table 10). Cells of most clusters expressed *PDCD1, TOX,* and *IFNG*, indicating their cognate activation (Fig. 5D). Synovial CD8$^+$CD45RO$^+$ T cells of cluster 1 represented 15.6% (11.6%-16.4%) of synovial CD8$^+$CD45RO$^+$ T cells and expressed both *CD8A* and *CD8B* and signature genes of T$_{RM}$ cells, such as *ITGA1* (CD49b), *DUSP6*, and *CXCR6* (Fig. 5D and E). Strikingly, these cells upregulated expression of the T$_h$ cell-associated genes *CD40LG, CSF2, IL21, TNF, KLRB1* (CD161), *ENTPD1* (CD39), *TNFRSF18* (GITR), *CXCL13*, and also the long-non-coding RNA *BHLHE40-AS1*. In this regard, they highly resembled pro-inflammatory CD4$^+$ Tcon of cluster 1. Accordingly, CD8$^+$CD45RO$^+$ T cells of cluster 1 also downregulated the expression of *EOMES, NKG7*, or genes encoding granzymes as compared to cells outside of cluster 1 (Fig. 5D and E). This was also true for the genes *CCR7, SELL, KLF2, S1PR1*, and *CXCR5* (Fig. 5D and E). Of note, PD-1^{high}CD8$^+$ T cells were enriched in inflamed joints of JIA patients compared to blood and were able to secrete the proteins IL-21 and GM-CSF (Supporting Information Fig. S10). Taken together, their distinct gene expression signature indicates that these cells *i)* are activated by antigen, and *ii)* are presumably an MHC class I-restricted CD8$^+$ "mirror

population" of pro-inflammatory synovial CD4$^+$ Tcon of cluster 1, and thus, cells with the potential to drive chronic inflammation.

Concluding Remarks

In summary, dissecting synovial effector T lymphocytes from patients with JIA using single-cell transcriptomics revealed an unforeseen heterogeneity and plasticity. Many of the cells express signature genes indicating continued activation by antigen *in situ* and transcribe genes encoding cytokines and chemokines with important functions in inflammation, such as *CSF2, IL21,* or *IL10*. Although clusters of T cells can be defined according to their transcriptional similarity, individual reaction patterns to antigenic stimulation differ, even within clusters. Of particular interest is a PD-1$^+$*TOX$^+$EOMES$^+$* population of CD4$^+$ T lymphocytes, representing clonally expanded, probably terminally differentiated, non-proliferating but very active effector T cells, potentially attracting myeloid cells, but also expressing *IL10* with the potential to regulate the immune reaction. These cells are also found in the circulation and might have the potential to limit the systemic spread of inflammation. In any case, they may serve as biomarkers to monitor JIA disease activity and response to therapy non-invasively. Two other populations of interest are a PD-1$^+$*TOX$^+$BHLHE40$^+$* population of CD4$^+$ T cells and a mirror population of CD8$^+$ T lymphocytes, presumably supporting extrafollicular B cell activation by secretion of IL-21 and CXCL13, as well as activation of myeloid cells by secretion of TNF and GM-CSF. These cells, too, are clonally expanded, non-proliferating, and terminally differentiated. The considerable individual heterogeneity of cells driving inflammation in various ways, and limiting it in others, provides a challenge for the development of effective targeted therapies that address these diverse cell types differentially and concomitantly, in order to be efficient. The presented data provide a basis for the development of biomarkers and targeted immune-modulating therapies for JIA and potentially other chronic inflammatory diseases.

Materials and methods

Human patient samples

Peripheral blood (PB) and synovial fluid (SF) samples of JIA patients were collected at the Department of Pediatric Pulmonology, Immunology and Critical Care Medicine, Division of Pediatric Rheumatology at Charité–Universitätsmedizin Berlin as approved by the ethics committee of the Charité–Universitätsmedizin Berlin (approval no. EA2/069/15), at the Pediatric Rheumatology Department at University Medical Center of Utrecht (The Netherlands) in accordance with the Institutional Review Board of the University Medical Center Utrecht (approval no. 11–499/C), and at the Meyer children's hospital, Florence, as approved by the Meyer children's hospital ethics committee (approval no. 184/2016). PB from healthy adult volunteers was obtained from the Mini Donor Service at University Medical

Center Utrecht. Samples were collected in compliance with the Declaration of Helsinki. Peripheral blood (PB) and synovial fluid (SF) was obtained via vein puncture or intravenous drip, and by therapeutic joint aspiration of the affected joints, respectively. Informed consent was obtained from all patients either directly or from parents/guardians. Intestinal biopsies of IBD patients were obtained from the Azienda Ospedaliero-Universitaria Careggi (AOUC), Florence, as approved by the ethics committee of AOUC hospital (approval no. 12382_BIO).

Isolation of antigen-experienced (memory) T cells from the SF and the PB of JIA patients for single-cell sequencing and qPCR analyses

Mononuclear cells from the peripheral blood (PBMCs) were isolated by Ficoll density-gradient centrifugation and subsequent collection of the leukocyte-containing interphase.

For the isolation of leukocytes from the synovial fluid, we diluted the viscous fluid with 5 mM ethylenediaminetetraacetic acid (EDTA)-containing PBS and filtered the cells using a 70 μm cell strainer (BD). Subsequently, cells were centrifuged at 300 g at 4°C and resuspended in PBS containing 0.2% BSA (PBS/BSA). Following an additional filtration step through a 70 μm cell strainer, cells were resuspended in PBS/BSA prior to depletion of CD15$^+$ neutrophils by magnetic cell separation (MACS, Miltenyi Biotec).

Single-cell suspensions of PBMCs and CD15-depleted SF cells were blocked with human FcR blocking reagent (Miltenyi Biotec) and labeled for 15 min at 4°C with antibodies for fluorescence-activated cell sorting (FACS) using a FACS-Aria II (BD). The following antibodies were used for labeling cells prior to FACS: anti-human CD3 Alexa Fluor 405 (AF405, clone UCHT1, DRFZ Berlin), CD4 Brilliant Violet 785 (BV785, EH12.2H7; Biolegend), CD45RO BV510 (clone UCHL1, BD), CD39 BV605 (clone A1, Biolegend), CD127 AF488 (clone A019D5, Biolegend), CD25 allophycocyanin (APC, M-A251, BD), CD8a APC-Cyanine 7 (APC-Cy7, clone: HIT8a, Biolegend), PD-1 PE-Cy7 (clone EH12.2H7, Biolegend), CD14 peridinin-chlorophyll protein complex (PerCP, clone TM1, DRFZ Berlin) and PI (Sigma–Aldrich).

Cells were sorted to obtain antigen-experienced (memory) CD4$^+$CD45RO$^+$CD25$^-$ T cells (Tcon), CD4$^+$CD45RO$^+$CD127^{lo}CD25$^+$ regulatory T cells (Treg), and CD8$^+$CD45RO$^+$ T cells as shown in Supporting Information Fig. S1. Sorted cells then were subjected to single-cell sequencing or qPCR following isolation of RNA.

Single-cell RNA-sequencing

For single-cell library preparation, FACS-sorted human T cells were applied to the 10X Genomics platform using the Chromium Single Cell 5' Library & Gel Bead Kit (10X Genomics) and following the manufacturer's instructions for capturing ~3000 cells.

The amplified cDNA was used for simultaneous 5' gene expression (GEX) and TCR library preparation. TCR target enrichment was achieved using the Chromium Single Cell V(D)J Enrichment Kit for Human T cells. Through fragmentation, adapter ligation and index PCR the final libraries were obtained. The quality of single cell 5' GEX and TCR libraries was assessed by Qubit quantification, Bioanalyzer fragment analysis (HS DNA Kit, Agilent), and KAPA library quantification qPCR (Roche). The sequencing was performed on a NextSeq 500 device (Illumina) using High Output v2 Kits (150 cycles) with the recommended sequencing conditions for 5' GEX libraries (read1: 26nt, read2: 98nt, index1: 8nt, index2: n.a.) and Mid Output v2 Kits (300 cycles) for TCR libraries (read1: 150nt, read2: 150nt, index1: 8nt, index2: n.a., 20% PhiX spike-in). Raw Illumina-NextSeq 500 data were processed using cellranger-2.1.1. Mkfastq, count commands, and vdj commands were used with default parameter settings. The genome reference was refdata-cellranger-hg19-1.2.0. The vdj-reference was refdata-cellranger-vdj-GRCh38-alts-ensembl-2.0.0. In both cases, the number of expected cells was set to 3000.

Quality control and filtering of single-cell transcriptomes

Single-cell RNA sequencing data were mapped as described above. The resulting expression matrix was analyzed in R using the Seurat package (version 3.1.1) following the principle steps described previously by Tallulah S. Andrews and Martin Hemberg [25]. In brief, putative artifacts from each sample were filtered by removing transcriptomes with less than 2500 and more than 12 500 transcripts and transcriptomes comprising less than 1% or more than 10% of mitochondrial transcripts. In addition, also the 1st and 95th percentile of transcriptomes, as judged by the fraction of mitochondrial transcripts, as well as the 5th and 95th percentile, as judged by the number of transcripts, were discarded. Subsequently, a preliminary t-distributed stochastic neighbor embedding (t-SNE) was performed for synovial and blood samples using *RunPCA and RuntSNE* functions with default parameter settings. By manual inspection, 54 cells were identified as monocytic contamination based on separate clustering and detection of marker transcripts (e.g., *CD14* and *ITGAM* among others, see cluster 6 shown in Supporting Information Fig. S2a) as well as a cluster representing FOXP3-expressing regulatory T cells (483 cells; cluster 5 shown in Fig. S2a) among synovial CD4$^+$CD45RO$^+$CD25$^-$ T cells. The respective clusters were removed from further analysis of synovial Tcon (Supporting Information Fig. S2b). The filtered set comprised six paired PB and SF samples with 13 479 and 12 481 Tcon, respectively. In addition, Tcon from patient 3 did not have a corresponding PB sample and included 1275 synovial Tcon (summing up to 13 756 synovial Tcon in total).

In addition, the filtered set contained 10 872 and 10 157 CD4$^+$CD45RO$^+$CD127^{lo}CD25$^+$ (Treg) cells, as well as 12 111 and 14 019 CD8$^+$CD45RO$^+$ T cells from the PB and the SF, respectively.

Single-cell transcriptome profiling

Single-cell transcriptome profiling was performed using the Seurat R package (version 3.1.1).

In particular, samples from the PB and the SF were filtered as described above and integrated (combined) with the functions *FindIntegrationAnchors* and *IntegrateData* as proposed by Rahul Satija and colleagues (Tim Stuart et al.) and thereby batch-corrected [77]. As input for the *FindIntegrationAnchors*, the 800 most variable features were determined within each sample. A list of unique variable features from different samples (SF Tcon, PB Tcon, SF Treg, PB Treg, SF CD8$^+$CD45RO$^+$ T cells, and PB CD8$^+$CD45RO$^+$ T cells) was supplied to the integration procedure. The integrated expression matrix was z-transformed by the *ScaleData* function and used to determine the first 50 principal components (PC) using *RunPCA*. Based on significant PCs (p-value < 0.001 as determined by *JackStraw* and *ScoreJackStraw*) t-distributed stochastic neighbor embedding was performed using *RuntSNE*, with a perplexity of 50 and a theta value of 0. Finally, communities of cells (clusters) were annotated by the functions *FindNeighbors* and *FindClusters* using the Louvain algorithm and were based on the significant PCs and a resolution of 0.2 [25].

Regarding gene expression displayed by heatmaps, the heatmap color scales indicate the row-wise z-scores of expression means (determined by Seurat's *AverageExpression*) of log-normalized (by Seurat's *LogNormalize*) UMIs per cluster (*RNA assay* used). For unsupervised heatmaps, significantly differentially expressed genes were selected as follows: The expression level of cells from one cluster was compared to the expression level of cells from all the other clusters using the *FindAllMarkers* function. The statistical test used was Wilcoxon's rank sum test. Only genes (features) were included that were expressed by at least 10% of cells in the respective cluster and which resulted in an adjusted p-value (Bonferroni correction) lower or equal to 0.05.

Cell-wise module scores for gene sets were generated by Seurat's *AddModuleScore* function with default parameters and using the RNA assay.

Feature plots (gene expression levels on t-SNE maps) show log normalized (Seurat's *LogNormalize* function) UMIs with a color scale cutoff at the 95th percentile.

Single-cell TCR repertoire profiling

The Immune-Profiling analysis by cellranger revealed 16 733 and 15 477 Tcon from six paired PB and SF samples, respectively, as well as additional 1628 cells from the SF from a donor whose blood sample was not sequenced. For further analysis, solely cells with annotations of the v(d)j gene and the cdr3 regions for both the TCR alpha and the TCR beta chain were considered. For cells with ambiguous alpha or beta chain annotations, contigs with the best quality, that is, productive-ness, full-length and highest number of reads and UMIs were chosen. Cells were integrated with the transcriptome analysis (including quality assessment and filtering), revealing 7098 out of 13 479 cells and 7403 out of 12 481 cells from six paired Tcon blood and synovial fluid samples, respectively, plus 1042 out of 1275 cells from synovial Tcon with no corresponding blood sample. For overlaps between PB and SF, cells with no corresponding blood sample were not considered. The clonotypes were defined by the donor origin, the v(d)j genes, and the cdr3nt annotations for both the TCR alpha and the TCR beta chain. Overlaps were defined by the ratio of cells in a cluster with clonotypes shared by a cluster being compared. Overlaps between two clusters were compared to overlaps between these two clusters with randomized cluster annotations. Overlaps of clusters were considered to be significant when not more than 5 out 1000 randomized overlaps were higher than the experimentally measured overlap of clusters.

Monocle trajectories, GSEA, and shortest-path analysis

In order to determine a pseudotime cell trajectory using the monocle-package (version 2.12) by Cole Trapnell, processed data had to be transferred from the Seurat object to monocle's CellDataSet object. The data provided to monocle were the expression matrix of Seurat's integrated assay. *ExpressionFamily* was set to "uninormal", since UMI-processing has been done in Seurat before. In *setOrderingFilter*, all genes of the integrated assay were selected as *ordering_genes*. In the function *reduceDimension*, parameter "norm_method" was set to "none", "reduction_method" set to "DDRTree", "pseudo_expr" to "0" and "max_components" set to "6". Other arguments were left default. Cells were then arranged by *orderCells* with default settings apart from manually setting the "root_state" to the state that mostly corresponded to Seurat's Cluster 0.

The gene set enrichment analysis (GSEA) was performed based on the CERNO test analog to the tmod R package using pre-ranked genes and Reactome pathways as gene sets [32, 78–80]. In particular, for each single cell, genes were ranked by the difference to the mean expression among all synovial Tcon. Gene sets with p-values ≤ 0.05 and a false discovery rate (FDR) ≤ 0.25 were considered as significant and projected onto the Monocle-based trajectory. Visualized are the area under the curve (AUC)-values for cells showing significant enrichment.

For the Shortest-Path analysis an undirected, weighted graph was generated for cells with common TCR annotations, based on Monocle and assuming that each cell could represent a reference intermediate state. Each cell was connected to its 10 nearest neighbors based on Euclidian distance. The Shortest-Path was computed for each pair using the Dijkstra algorithm. The importance of a cell was judged by the Betweenness-Centrality. Significant paths between cells with a Betweenness-Centrality greater than $0.1 * n * (n - 1)$, with n being the number of cells, were visualized. The direction of an edge was judged by the higher centrality value.

Statistical analyses

All statistical tests are specified in the figure legends of the respective analyses, as well as in the respective material and methods

section. Statistical calculations were performed with GraphPad Prism version 5.04/7.04 and R version 3.6.1 if not specified otherwise. The following R packages were used for analyzing and for plotting data in this manuscript: RStudio (version 1.1.463), dplyr (version 0.8.3), forcats (version 0.4.0), ggplot2 (version 3.2.1), purrr (version 0.3.3), readr (version 1.3.1), stringr (version 1.4.0), tibble (version 2.1.3), tidyr (version 1.0.0), cowplot (version 1.0.0), Seurat (version 3.1.2), ggrepel (version 0.8.1), wesanderson (version 0.3.6), colorRamps (version 2.3), ggpubr (version 0.2.4), reshape2 (version 1.4.3), and monocle (version 2.12.0).

Conflict of Interest: The authors declare no commercial or financial conflict of interest.

Peer review: The peer review history for this article is available at https://publons.com/publon/10.1002/eji.202048797.

Data availability statement: Single-cell transcriptome and immune profiling data discussed in this publication, are available at gene expression omnibus (GEO) under the accession number GSE160097.

References

1 **Prakken, B.**, **Albani, S.** and **Martini, A.**, Juvenile idiopathic arthritis. *Lancet*. 2011. **377**: 2138–2149.

2 **Uhlig, H. H.** and **Powrie, F.**, Translating immunology into therapeutic concepts for inflammatory bowel disease. *Annu. Rev. Immunol.* 2018. **36**: 755–781.

3 **Cotsapas, C.**, **Mitrovic, M.** and **Hafler, D.**, Multiple sclerosis. *Handb Clin Neurol.* 2018. **148**: 723–730.

4 **Van Boxel, J. A.** and **Paget, S. A.**, Predominantly T-cell infiltrate in rheumatoid synovial membranes. *N. Engl. J. Med.* 1975. **293**: 517–520.

5 **Shale, M.**, **Schiering, C.** and **Powrie, F.**, CD4(+) T-cell subsets in intestinal inflammation. *Immunol. Rev.* 2013. **252**: 164–182.

6 **Abraham, C.** and **Cho, J. H.**, Inflammatory bowel disease. *N. Engl. J. Med.* 2009. **361**: 2066–2078.

7 **Wedderburn, L. R.**, **Robinson, N.**, **Patel, A.**, **Varsani, H.** and **Woo, P.**, Selective recruitment of polarized T cells expressing CCR5 and CXCR3 to the inflamed joints of children with juvenile idiopathic arthritis. *Arthritis Rheum.* 2000. **43**: 765–774.

8 **Hinks, A.**, **Worthington, J.** and **Thomson, W.**, The association of PTPN22 with rheumatoid arthritis and juvenile idiopathic arthritis. *Rheumatology (Oxford)* 2006. **45**: 365–368.

9 **Diogo, D.**, **Okada, Y.** and **Plenge, R. M.**, Genome-wide association studies to advance our understanding of critical cell types and pathways in rheumatoid arthritis: recent findings and challenges. *Curr. Opin. Rheumatol.* 2014. **26**: 85–92.

10 **Gutierrez-Arcelus, M.**, **Rich, S. S.** and **Raychaudhuri, S.**, Autoimmune diseases - connecting risk alleles with molecular traits of the immune system. *Nat. Rev. Genet.* 2016. **17**: 160–174.

11 **Raychaudhuri, S.**, Recent advances in the genetics of rheumatoid arthritis. *Curr. Opin. Rheumatol.* 2010. **22**: 109–118.

12 **Becher, B.**, **Tugues, S.** and **Greter, M.**, GM-CSF: from growth factor to central mediator of tissue inflammation. *Immunity* 2016. **45**: 963–973.

13 **Rao, D. A.**, **Gurish, M. F.**, **Marshall, J. L.**, **Slowikowski, K.**, **Fonseka, C. Y.**, **Liu, Y.**, **Donlin, L. T.** et al., Pathologically expanded peripheral T helper cell subset drives B cells in rheumatoid arthritis. *Nature* 2017. **542**: 110–114.

14 **Burmester, G. R.**, **Feist, E.**, **Sleeman, M. A.**, **Wang, B.**, **White, B.** and **Magrini, F.**, Mavrilimumab, a human monoclonal antibody targeting GM-CSF receptor-alpha, in subjects with rheumatoid arthritis: a randomised, double-blind, placebo-controlled, phase I, first-in-human study. *Ann. Rheum. Dis.* 2011. **70**: 1542–1549.

15 **Burmester, G. R.**, **Weinblatt, M. E.**, **McInnes, I. B.**, **Porter, D.**, **Barbarash, O.**, **Vatutin, M.**, **Szombati, I.** et al., Efficacy and safety of mavrilimumab in subjects with rheumatoid arthritis. *Ann. Rheum. Dis.* 2013. **72**: 1445–1452.

16 **Cook, A. D.** and **Hamilton, J. A.**, Investigational therapies targeting the granulocyte macrophage colony-stimulating factor receptor-alpha in rheumatoid arthritis: focus on mavrilimumab. *Ther Adv Musculoskelet Dis* 2018. **10**: 29–38.

17 **Noster, R.**, **Riedel, R.**, **Mashreghi, M. F.**, **Radbruch, H.**, **Harms, L.**, **Haftmann, C.**, **Chang, H. D.** et al., IL-17 and GM-CSF expression are antagonistically regulated by human T helper cells. *Sci. Transl. Med.* 2014. **6**: 241ra280.

18 **Codarri, L.**, **Gyulveszi, G.**, **Tosevski, V.**, **Hesske, L.**, **Fontana, A.**, **Magnenat, L.**, **Suter, T.** et al., RORgammat drives production of the cytokine GM-CSF in helper T cells, which is essential for the effector phase of autoimmune neuroinflammation. *Nat. Immunol.* 2011. **12**: 560–567.

19 **Fischer, D. S.**, **Wu, Y.**, **Schubert, B.** and **Theis, F. J.**, Predicting antigen-specificity of single T-cells based on TCR CDR3 regions. *bioRxiv [Preprint]* 2019: 734053.

20 **Jurtz, V. I.**, **Jessen, L. E.**, **Bentzen, A. K.**, **Jespersen, M. C.**, **Mahajan, S.**, **Vita, R.**, **Jensen, K. K.** et al., NetTCR: sequence-based prediction of TCR binding to peptide-MHC complexes using convolutional neural networks. *bioRxiv* 2018: 433706.

21 **Gielis, S.**, **Moris, P.**, **Bittremieux, W.**, **De Neuter, N.**, **Ogunjimi, B.**, **Laukens, K.** and **Meysman, P.**, Detection of Enriched T Cell Epitope Specificity in Full T Cell Receptor Sequence Repertoires. *Frontiers in Immunology* 2019. **10**.

22 **Ogishi, M.** and **Yotsuyanagi, H.**, Quantitative Prediction of the Landscape of T Cell Epitope Immunogenicity in Sequence Space. *Frontiers in Immunology* 2019. **10**.

23 **Westendorf, K.**, **Okhrimenko, A.**, **Grun, J. R.**, **Schliemann, H.**, **Chang, H. D.**, **Dong, J.** and **Radbruch, A.**, Unbiased transcriptomes of resting human CD4(+) CD45RO(+) T lymphocytes. *Eur. J. Immunol.* 2014. **44**: 1866–1869.

24 **Cossarizza, A.**, **Chang, H. D.**, **Radbruch, A.**, **Acs, A.**, **Adam, D.**, **Adam-Klages, S.**, **Agace, W. W.** et al., Guidelines for the use of flow cytometry and cell sorting in immunological studies (second edition). *Eur. J. Immunol.* 2019. **49**: 1457–1973.

25 **Andrews, T. S.** and **Hemberg, M.**, Identifying cell populations with scR-NASeq. *Mol. Aspects Med.* 2018. **59**: 114–122.

26 **Tirosh, I.**, **Izar, B.**, **Prakadan, S. M.**, **Wadsworth, M. H., 2nd**, **Treacy, D.**, **Trombetta, J. J.**, **Rotem, A.** et al., Dissecting the multicellular ecosystem of metastatic melanoma by single-cell RNA-seq. *Science* 2016. **352**: 189–196.

27 **Cyster, J. G.** and **Schwab, S. R.**, Sphingosine-1-phosphate and lymphocyte egress from lymphoid organs. *Annu. Rev. Immunol.* 2012. **30**: 69–94.

28 **Sallusto, F.**, **Lenig, D.**, **Forster, R.**, **Lipp, M.** and **Lanzavecchia, A.**, Two subsets of memory T lymphocytes with distinct homing potentials and effector functions. *Nature* 1999. **401**: 708–712.

29 **Abbas, A. R.**, **Wolslegel, K.**, **Seshasayee, D.**, **Modrusan, Z.** and **Clark, H. F.**, Deconvolution of blood microarray data identifies cellular activation patterns in systemic lupus erythematosus. *PLoS One* 2009. **4**: e6098.

30 **Ko, H. S.**, **Fu, S. M.**, **Winchester, R. J.**, **Yu, D. T.** and **Kunkel, H. G.**, Ia determinants on stimulated human T lymphocytes. Occurrence on mitogen- and antigen-activated T cells. *J. Exp. Med.* 1979. **150**: 246–255.

31 **Holling, T. M.**, **Schooten, E.** and **van Den Elsen, P. J.**, Function and regulation of MHC class II molecules in T-lymphocytes: of mice and men. *Hum. Immunol.* 2004. **65**: 282–290.

32 **Fabregat, A.**, **Jupe, S.**, **Matthews, L.**, **Sidiropoulos, K.**, **Gillespie, M.**, **Garapati, P.**, **Haw, R.** et al., The Reactome Pathway Knowledgebase. *Nucleic. Acids. Res.* 2018. **46**: D649–D655.

33 **Frentsch, M.**, **Arbach, O.**, **Kirchhoff, D.**, **Moewes, B.**, **Worm, M.**, **Rothe, M.**, **Scheffold, A.** et al., Direct access to CD4+ T cells specific for defined antigens according to CD154 expression. *Nat. Med.* 2005. **11**: 1118–1124.

34 **Bacher, P.**, **Heinrich, F.**, **Stervbo, U.**, **Nienen, M.**, **Vahldieck, M.**, **Iwert, C.**, **Vogt, K.** et al., Regulatory T Cell Specificity Directs Tolerance versus Allergy against Aeroantigens in Humans. *Cell* 2016. **167**: 1067–1078 e1016.

35 **Siracusa, F.**, **Durek, P.**, **McGrath, M. A.**, **Sercan-Alp, O.**, **Rao, A.**, **Du, W.**, **Cendon, C.** et al., CD69(+) memory T lymphocytes of the bone marrow and spleen express the signature transcripts of tissue-resident memory T lymphocytes. *Eur. J. Immunol.* 2019. **49**: 966–968.

36 **Kumar, B. V.**, **Ma, W.**, **Miron, M.**, **Granot, T.**, **Guyer, R. S.**, **Carpenter, D. J.**, **Senda, T.** et al., Human Tissue-Resident Memory T Cells Are Defined by Core Transcriptional and Functional Signatures in Lymphoid and Mucosal Sites. *Cell Rep.* 2017. **20**: 2921–2934.

37 **Mackay, L. K.**, **Minnich, M.**, **Kragten, N. A.**, **Liao, Y.**, **Nota, B.**, **Seillet, C.**, **Zaid, A.** et al., Hobit and Blimp1 instruct a universal transcriptional program of tissue residency in lymphocytes. *Science* 2016. **352**: 459–463.

38 **Zundler, S.**, **Becker, E.**, **Spocinska, M.**, **Slawik, M.**, **Parga-Vidal, L.**, **Stark, R.**, **Wiendl, M.** et al., Hobit- and Blimp-1-driven CD4(+) tissue-resident memory T cells control chronic intestinal inflammation. *Nat. Immunol.* 2019. **20**: 288–300.

39 **Iijima, N.** and **Iwasaki, A.**, T cell memory. A local macrophage chemokine network sustains protective tissue-resident memory CD4 T cells. *Science* 2014. **346**: 93–98.

40 **Korn, T.**, **Bettelli, E.**, **Oukka, M.** and **Kuchroo, V. K.**, IL-17 and Th17 Cells. *Annu. Rev. Immunol.* 2009. **27**: 485–517.

41 **Nowak, A.**, **Lock, D.**, **Bacher, P.**, **Hohnstein, T.**, **Vogt, K.**, **Gottfreund, J.**, **Giehr, P.** et al., CD137+CD154- Expression As a Regulatory T Cell (Treg)-Specific Activation Signature for Identification and Sorting of Stable Human Tregs from In Vitro Expansion Cultures. *Front. Immunol.* 2018. **9**: 199.

42 **Takeuchi, A.**, **Badr Mel, S.**, **Miyauchi, K.**, **Ishihara, C.**, **Onishi, R.**, **Guo, Z.**, **Sasaki, Y.** et al., CRTAM determines the CD4+ cytotoxic T lymphocyte lineage. *J. Exp. Med.* 2016. **213**: 123–138.

43 **Gruarin, P.**, **Maglie, S.**, **De Simone, M.**, **Haringer, B.**, **Vasco, C.**, **Ranzani, V.**, **Bosotti, R.** et al., Eomesodermin controls a unique differentiation program in human IL-10 and IFN-gamma coproducing regulatory T cells. *Eur. J. Immunol.* 2019. **49**: 96–111.

44 **Zhang, P.**, **Lee, J. S.**, **Gartlan, K. H.**, **Schuster, I. S.**, **Comerford, I.**, **Varelias, A.**, **Ullah, M. A.** et al., Eomesodermin promotes the development of type 1 regulatory (TR1) cells. *Sci Immunol* 2017. **2**.

45 **Gregori, S.**, **Goudy, K. S.** and **Roncarolo, M. G.**, The cellular and molecular mechanisms of immuno-suppression by human type 1 regulatory T cells. *Front. Immunol.* 2012. **3**: 30.

46 **Yang, Y. H.**, **Song, W.**, **Deane, J. A.**, **Kao, W.**, **Ooi, J. D.**, **Ngo, D.**, **Kitching, A. R.** et al., Deficiency of annexin A1 in CD4+ T cells exacerbates T cell-dependent inflammation. *J. Immunol.* 2013. **190**: 997–1007.

47 **D'Acquisto, F.**, **Merghani, A.**, **Lecona, E.**, **Rosignoli, G.**, **Raza, K.**, **Buckley, C. D.**, **Flower, R. J.** et al., Annexin-1 modulates T-cell activation and differentiation. *Blood* 2007. **109**: 1095–1102.

48 **D'Acquisto, F.**, **Paschalidis, N.**, **Sampaio, A. L.**, **Merghani, A.**, **Flower, R. J.** and **Perretti, M.**, Impaired T cell activation and increased Th2 lineage commitment in Annexin-1-deficient T cells. *Eur. J. Immunol.* 2007. **37**: 3131–3142.

49 **Baaten, B. J.**, **Li, C. R.**, **Deiro, M. F.**, **Lin, M. M.**, **Linton, P. J.** and **Bradley, L. M.**, CD44 regulates survival and memory development in Th1 cells. *Immunity* 2010. **32**: 104–115.

50 **Shaffer, M. H.**, **Dupree, R. S.**, **Zhu, P.**, **Saotome, I.**, **Schmidt, R. F.**, **McClatchey, A. I.**, **Freedman, B. D.** et al., Ezrin and moesin function together to promote T cell activation. *J. Immunol.* 2009. **182**: 1021–1032.

51 **Aleem, E.**, **Kiyokawa, H.** and **Kaldis, P.**, Cdc2-cyclin E complexes regulate the G1/S phase transition. *Nat. Cell Biol.* 2005. **7**: 831–836.

52 **Diril, M. K.**, **Ratnacaram, C. K.**, **Padmakumar, V. C.**, **Du, T.**, **Wasser, M.**, **Coppola, V.**, **Tessarollo, L.** et al., Cyclin-dependent kinase 1 (Cdk1) is essential for cell division and suppression of DNA re-replication but not for liver regeneration. *Proc. Natl. Acad. Sci. U. S. A.* 2012. **109**: 3826–3831.

53 **Scholzen, T.** and **Gerdes, J.**, The Ki-67 protein: from the known and the unknown. *J. Cell. Physiol.* 2000. **182**: 311–322.

54 **Trapnell, C.**, **Cacchiarelli, D.**, **Grimsby, J.**, **Pokharel, P.**, **Li, S.**, **Morse, M.**, **Lennon, N. J.** et al., The dynamics and regulators of cell fate decisions are revealed by pseudotemporal ordering of single cells. *Nat. Biotechnol.* 2014. **32**: 381–386.

55 **Alfei, F.**, **Kanev, K.**, **Hofmann, M.**, **Wu, M.**, **Ghoneim, H. E.**, **Roelli, P.**, **Utzschneider, D. T.** et al., TOX reinforces the phenotype and longevity of exhausted T cells in chronic viral infection. *Nature* 2019. **571**: 265–269.

56 **Khan, O.**, **Giles, J. R.**, **McDonald, S.**, **Manne, S.**, **Ngiow, S. F.**, **Patel, K. P.**, **Werner, M. T.** et al., TOX transcriptionally and epigenetically programs CD8(+) T cell exhaustion. *Nature* 2019. **571**: 211–218.

57 Scott, A. C., Dundar, F., Zumbo, P., Chandran, S. S., Klebanoff, C. A., Shak-iba, M., Trivedi, P. et al., TOX is a critical regulator of tumour-specific T cell differentiation. *Nature* 2019. **571**: 270–274.

58 Niesner, U., Albrecht, I., Janke, M., Doebis, C., Loddenkemper, C., Lexberg, M. H., Eulenburg, K. et al., Autoregulation of Th1-mediated inflammation by twist1. *J. Exp. Med.* 2008. **205**: 1889–1901.

59 Pearce, E. L., Mullen, A. C., Martins, G. A., Krawczyk, C. M., Hutchins, A. S., Zediak, V. P., Banica, M. et al., Control of effector CD8+ T cell function by the transcription factor Eomesodermin. *Science* 2003. **302**: 1041–1043.

60 Mazzoni, A., Maggi, L., Siracusa, F., Ramazzotti, M., Rossi, M. C., San-tarlasci, V., Montaini, G. et al., Eomes controls the development of Th17-derived (non-classic) Th1 cells during chronic inflammation. *Eur. J. Immunol.* 2019. **49**: 79–95.

61 Maschmeyer, P., Petkau, G., Siracusa, F., Zimmermann, J., Zugel, F., Kuhl, A. A., Lehmann, K. et al., Selective targeting of pro-inflammatory Th1 cells by microRNA-148a-specific antagomirs in vivo. *J. Autoimmun.* 2018. **89**: 41–52.

62 Hradilkova, K., Maschmeyer, P., Westendorf, K., Schliemann, H., Husak, O., von Stuckrad, A. S. L., Kallinich, T. et al., Regulation of Fatty Acid Oxi-dation by Twist 1 in the Metabolic Adaptation of T Helper Lymphocytes to Chronic Inflammation. *Arthritis Rheumatol* 2019. **71**: 1756–1765.

63 Haftmann, C., Stittrich, A. B., Zimmermann, J., Fang, Z., Hradilkova, K., Bardua, M., Westendorf, K. et al., miR-148a is upregulated by Twist1 and T-bet and promotes Th1-cell survival by regulating the proapoptotic gene Bim. *Eur. J. Immunol.* 2015. **45**: 1192–1205.

64 Christophersen, A., Lund, E. G., Snir, O., Sola, E., Kanduri, C., Dahal-Koirala, S., Zuhlke, S. et al., Distinct phenotype of CD4(+) T cells driv-ing celiac disease identified in multiple autoimmune conditions. *Nat. Med.* 2019. **25**: 734–737.

65 Jain, A., Irizarry-Caro, R. A., McDaniel, M. M., Chawla, A. S., Carroll, K. R., Overcast, G. R., Philip, N. H. et al., T cells instruct myeloid cells to pro-duce inflammasome-independent IL-1beta and cause autoimmunity. *Nat. Immunol.* 2020. **21**: 69.

66 Hamilton, J. A., GM-CSF in inflammation. *J. Exp. Med.* 2020. **217**.

67 Gunn, M. D., Ngo, V. N., Ansel, K. M., Ekland, E. H., Cyster, J. G. and Williams, L. T., A B-cell-homing chemokine made in lymphoid follicles activates Burkitt's lymphoma receptor-1. *Nature* 1998. **391**: 799–803.

68 Rao, D. A., T Cells That Help B Cells in Chronically Inflamed Tissues. *Front. Immunol.* 2018. **9**: 1924.

69 Gandhi, R., Kumar, D., Burns, E. J., Nadeau, M., Dake, B., Laroni, A., Kozoriz, D. et al., Activation of the aryl hydrocarbon receptor induces human type 1 regulatory T cell-like and Foxp3(+) regulatory T cells. *Nat. Immunol.* 2010. **11**: 846–853.

70 Grossman, W. J., Verbsky, J. W., Tollefsen, B. L., Kemper, C., Atkinson, J. P. and Ley, T. J., Differential expression of granzymes A and B in human cytotoxic lymphocyte subsets and T regulatory cells. *Blood* 2004. **104**: 2840–2848.

71 Zimmermann, J., Kuhl, A. A., Weber, M., Grun, J. R., Loffler, J., Haft-mann, C., Riedel, R. et al., T-bet expression by Th cells promotes type 1 inflammation but is dispensable for colitis. *Mucosal Immunol* 2016. **9**: 1487–1499.

72 Lin, C. C., Bradstreet, T. R., Schwarzkopf, E. A., Sim, J., Carrero, J. A., Chou, C., Cook, L. E. et al., Bhlhe40 controls cytokine production by T cells and is essential for pathogenicity in autoimmune neuroinflammation. *Nat. Commun.* 2014. **5**: 3551.

73 Huynh, J. P., Lin, C. C., Kimmey, J. M., Jarjour, N. N., Schwarzkopf, E. A., Bradstreet, T. R., Shchukina, I. et al., Bhlhe40 is an essential repressor of IL-10 during Mycobacterium tuberculosis infection. *J. Exp. Med.* 2018. **215**: 1823–1838.

74 Martinez-Llordella, M., Esensten, J. H., Bailey-Bucktrout, S. L., Lipsky, R. H., Marini, A., Chen, J., Mughal, M. et al., CD28-inducible transcription factor DEC1 is required for efficient autoreactive CD4+ T cell response. *J. Exp. Med.* 2013. **210**: 1603–1619.

75 Emming, S., Bianchi, N., Polletti, S., Balestrieri, C., Leoni, C., Montagner, S., Chirichella, M. et al., A molecular network regulating the proinflam-matory phenotype of human memory T lymphocytes. *Nat. Immunol.* 2020. **21**: 388–399.

76 Petrelli, A., Mijnheer, G., Hoytema van Konijnenburg, D. P., van der Wal, M. M., Giovannone, B., Mocholi, E., Vazirpanah, N. et al., PD-1+CD8+ T cells are clonally expanding effectors in human chronic inflammation. *J. Clin. Invest.* 2018. **128**: 4669–4681.

77 Stuart, T., Butler, A., Hoffman, P., Hafemeister, C., Papalexi, E., Mauck, W. M., 3rd, Hao, Y. et al., Comprehensive Integration of Single-Cell Data. *Cell* 2019. **177**: 1888–1902 e1821.

78 Weiner, J. and Domaszewska, T., tmod: an R package for general and mul-tivariate enrichment analysis 2016.

79 Yamaguchi, K. D., Ruderman, D. L., Croze, E., Wagner, T. C., Velichko, S., Reder, A. T. and Salamon, H., IFN-beta-regulated genes show abnormal expression in therapy-naive relapsing-remitting MS mononuclear cells: gene expression analysis employing all reported protein-protein interac-tions. *J. Neuroimmunol.* 2008. **195**: 116–120.

80 Zyla, J., Marczyk, M., Domaszewska, T., Kaufmann, S. H. E., Polanska, J. and Weiner, J., Gene set enrichment for reproducible science: comparison of CERNO and eight other algorithms. *Bioinformatics* 2019.

Abbreviations: **CID:** chronic inflammatory disease · **JIA:** juvenile idiopathic arthritis · **IBD:** inflammatory bowel disease · **Tcon:** con-ventional CD4$^+$ T lymphocyte · **TCR:** T cell receptor

Full correspondence: Dr. Mir-Farzin Mashreghi, Deutsches Rheuma-Forschungszentrum (DRFZ), an Institute of the Leibniz Association, Charitéplatz 1, 10117 Berlin, Germany.
e-mail: mashreghi@drfz.de

Additional correspondence: Dr. Pawel Durek, Deutsches Rheuma-Forschungszentrum (DRFZ), an Institute of the Leibniz Association, Charitéplatz 1, 10117 Berlin, Germany.
e-mail: pawel.durek@drfz.de